Geoderma 307 (2017) 238–252

Contents lists available at ScienceDirect

Geoderma

journal homepage: www.elsevier.com/locate/geoderma

Redistribution of soil metals and organic carbon via lateral flowpaths at the catchment scale in a glaciated upland setting

Rebecca R. Bourgault[a,*], Donald S. Ross[a], Scott W. Bailey[b], Thomas D. Bullen[c], Kevin J. McGuire[d], John P. Gannon[e]

[a] Dept. of Plant and Soil Science, University of Vermont, Jeffords Hall, Burlington, VT 05405, United States
[b] Center for Research on Ecosystem Change, US Forest Service, 234 Mirror Lake Rd., North Woodstock, NH 03262, United States
[c] US Geological Survey, Water Mission Area, MS 420, 345 Middlefield Rd., Menlo Park, CA 94025, United States
[d] Department of Forest Resources and Environmental Conservation and Virginia Water Resources Research Center, Virginia Tech, Blacksburg, VA 24061, United States
[e] Dept. of Geosciences & Natural Resources, Western Carolina University, 331 Stillwell Bldg. Cullowhee, NC 28723, United States

ARTICLE INFO

Handling Editor: M. Vepraskas

Keywords:
Podzols
Hydropedology
Organic carbon
Rare earth elements
Trace metals

ABSTRACT

Emerging evidence shows that interactions between soils and subsurface flow paths contribute to spatial variations in stream water chemistry in headwater catchments. However, few have yet attempted to quantify chemical variations in soils at catchment and hillslope scales. Watershed 3 (WS3) at Hubbard Brook Experimental Forest, New Hampshire, USA, was studied in order to better understand pedogenesis and its relationship to subsurface water dynamics. In WS3, 99 soil profiles were described, sampled by horizon, and assigned to a hydropedologic unit (HPU), a functional classification previously developed using landscape and morphological metrics which corresponded with distinct water table regimes. Soil samples were extracted with 1) citrate-dithionite (d) and analyzed for Fe_d and Mn_d; and 2) acid ammonium oxalate (o) and analyzed for Al_o, Fe_o and the rare earth elements La_o, Ce_o, and Pr_o. Total organic C was also measured. These elements were redistributed via vertical and lateral podzolization. Typical (horizontally layered) podzols developed in the majority of the catchment due to predominantly vertical, unsaturated flow. However, lateral flow produced four other podzol types with distinct chemistry; thicker spodic horizons of laterally accumulating soils generally reflected larger pools of trace metals and subsoil organic C. The spatial distribution of positive cerium-anomalies (Ce/Ce*) in soil profiles proved to be a consistent hydropedologic indicator of lateral flow and seasonally high water table in three hillslopes. Despite occasional high water table in some of the HPUs, they were not hydric soils and were distinct from wetter podzols of coastal plains due to their high Fe content. This study suggests that vertical and lateral spatial variation in soil chemical composition, including the complexity of Ce distribution, as it relates to subsurface water dynamics should be considered when studying or predicting catchment scale functions such as stream solute export and biogeochemical processes.

1. Introduction

Pedologists have long recognized that soil variations exist in all dimensions and scales even though they often study soils at the pedon scale, observing horizontal layers in cross-section. This has led to the implicit assumption of vertical water flow and therefore vertical horizon development. However, in many situations, especially in steep landscapes, soils can develop laterally as well as vertically because solutes can be translocated downslope along the predominant water flow path direction (Sommer, 2006). Lateral flow may arise from saturation development and permeability contrasts in soil or from wetting/drying hysteric effects in unsaturated sloping soils (McCord et al., 1991; Torres et al., 1998; Sinai and Dirksen, 2006). The main factors contributing to lateral flow in soils are a humid climate combined with steep slopes, sharp permeability contrasts at shallow depths, and generally coarse soil textures (Zaslavsky and Rogowski, 1969; Weiler et al., 2006; Lin, 2010). Lateral flow transports solutes downslope, where they may precipitate and accumulate some distance from where they were generated. For example, there are documented cases of lateral flow causing downslope accumulation in secondary Al oxides (Park and Burt, 2002; Löfgren and Cory, 2010; Lucas et al., 2012), Fe oxides (Park and Burt, 1999; Park and Burt, 2002; Fiedler et al., 2002),

Abbreviations: AOC, amorphous organometallic complexes; HBEF, Hubbard Brook Experimental Forest; HPU, hydropedologic unit; WS3, Watershed 3

* Corresponding author at: Dept. of Landscape Architecture and Environmental Sciences, Delaware Valley University, 700 E. Butler Ave., Doylestown, PA 18901, United States.
E-mail address: rebecca.bourgault@delval.edu (R.R. Bourgault).

http://dx.doi.org/10.1016/j.geoderma.2017.05.039
Received 11 February 2017; Received in revised form 18 May 2017; Accepted 19 May 2017

Mn oxides (McDaniel et al., 1992; Park and Burt, 1999; Park and Burt, 2002; Fiedler et al., 2002), clay (Mapa and Pathmarajah, 2007; Lucas et al., 2012), dissolved organic C (Fiedler et al., 2002), and amorphous organometallic complexes (AOC; Sommer et al., 2001; Park and Burt, 2002; Bardy et al., 2008; Buurman et al., 2013a,b; Jankowski, 2014).

Podzolization, the process leading to the formation of podzols, consists of chelation and illuviation of Al and organic matter, with or without Fe, from eluvial to illuvial horizons (McKeague et al., 1983). Traditionally, research in podzolization has also focused on vertical pedogenesis of individual pedons (e.g., Feldman et al., 1991; Freeland and Evans, 1993; Li et al., 1998; Melkerud et al., 2000). However, there are a few allusions to landscape scale processes and podzolization, including lateral subsurface translocation of Fe and Al (Blume and Schwertmann, 1969; Feldman et al., 1991). Lateral podzolization was explicitly documented by Sommer et al. (2001), who reported two morphologically distinct soil end-members that occurred in predictable topographic locations as a result of lateral transport and accumulation of spodic materials (i.e., amorphous compounds of organic matter, Al, and Fe). Recently, Bailey et al. (2014), Gannon et al. (2014), Bourgault et al. (2015a), and Gillin et al. (2015) documented similar morphological patterns and lateral podzolization in Watershed 3 (WS3) at the Hubbard Brook Experimental Forest, New Hampshire, USA. These studies identified and mapped hydropedologic units (HPUs), which are defined as groupings of pedons with similar morphology developed by influence of specific soil-forming factors: water table regime, flow paths, and saturation (Gannon et al., 2014). The HPUs classified at HBEF embodied differing vertical and lateral podzolization processes. The documentation of unsaturated lateral flux provided a hydrologic basis for the observed morphology and lateral podzolization which had previously been assumed (Gannon et al., 2017).

Within a typical podzol profile, vertical distribution and chemistry of secondary Al, Fe, and Mn species and organic C show predictable trends (Blume and Schwertmann, 1969). Surface (O and/or A) horizons tend to be leached of Al and Fe, while Mn tends to be highest in the surface due to biocycling by vegetation. The E horizon contains a minimum of Al, Fe, and Mn for the pedon due to eluviation. The Fe maximum tends to occur immediately below the E horizon, in the upper part of the spodic horizon, where Fe-organic complexes precipitate. Aluminum has a higher solubility than Fe in acid soils, and therefore the Al maximum occurs below the Fe maximum, in the lower part of the spodic horizon. Organic matter (OM) in the spodic horizon is different from that in the forest floor. B horizon OM tends to be more resistant to decomposition than OM in the soil surface, in part due to the stabilizing effect of chelation and/or sorption by Al, Fe and Mn, i.e. AOC (Buurman and Jongmans, 2005).

The stability of C sequestered in spodic horizons could potentially be affected by alteration of hydrologic conditions due to climate change. Most climate change models predict an increase in precipitation over North America (Dore, 2005), including Hubbard Brook (Dib et al., 2014). This scenario could lead to more frequent and sustained groundwater incursions into the solum and subsequent development of reducing conditions, which would destabilize Fe-OM complexes and export associated organic matter to the stream as dissolved organic carbon (DOC). Another possible mechanism for mobilizing organometallic complexes in these sloping, acid soils is an increase in soil acidification due to an increase in precipitation. Most climate change models also predict an increase in temperature, CO_2 and vegetative growth (Dore, 2005); these conditions could cause addition of greater amounts of soluble organic matter to pre-existing amorphous organometallic complexes, increasing solubility of these complexes (Buurman, 1985) and exporting stored C as DOC. On the other hand, the resulting increase in evapotranspiration could offset the increase in rainfall and actually reduce the volume of water entering streams (Huntington, 2003). This scenario would lower water tables, limit lateral podzolization, and may actually enhance decomposition of laterally deposited spodic materials by addition of O_2 deeper in the soil profile. Dib et al. (2014) showed that vegetative response to various climate change scenarios could have large effects on the source/ sink behavior of Hubbard Brook soils. The authors showed that if vegetative growth was enhanced, then the soils would be a C sink; if vegetation acclimated to the enhanced CO_2, then the soils would export C from the more resistant to more labile fractions and ultimately lose up to 30% C by 2099. The implications of these effects are important globally in podzolized regions, highlighting the importance of understanding the spatial variability in soil C due to hydropedologic processes.

Podzols can be developed by both vertical and lateral translocations. Lateral flow paths can be documented by observing landscape-scale distributions of specific mobile elements or soil materials, which act as tracers of dominant hydrologic pathways. Manganese tends to be more mobile than Fe in soils, and the ratio of citrate-dithionite extractable Mn (Mn_d) to citrate-dithionite-extractable Fe (Fe_d) has been used as an indicator of lateral flow at the landscape scale (McDaniel et al., 1992). The ratio of oxalate-extractable Fe (Fe_o) to dithionite-extractable Fe (Fe_d), termed the “Fe active ratio” (i.e. amorphous Fe oxides:total secondary oxides), has also been proposed as an indicator of lateral flow and lateral podzolization (Park and Burt, 1999, 2002). For example, Park and Burt (2002) documented a downslope increase in Mn_d/Fe_d, Fe_o/Fe_d and total secondary oxides of Fe, Al, and Mn on a podzolized slope, which the authors attributed to lateral flow and redistribution of AOC from upslope. Another suite of elements that have been considered as tracers of pedogenic processes is the rare earth elements (REEs) (Laveuf and Cornu, 2009). Chemical weathering releases REEs from primary minerals, which then become selectively adsorbed on or incorporated into secondary Mn and Fe oxides, clays, soil organic matter, and spodic materials. Poorly crystalline or amorphous soil minerals are better at retaining REEs than well-crystalline minerals (Land et al., 1999). Cerium is the only REE that occurs in the quadrivalent and trivalent states, while other REEs occur only in the trivalent state in soil environments. Some soils show a positive Ce-anomaly (Ce/Ce*), where Ce = actual Ce concentration and Ce* = expected Ce concentration given the concentrations of other REEs. A positive Ce-anomaly can develop passively as a result of preferential sorption of Ce on Fe and Mn oxide surfaces, while other REEs are leached (Murray et al., 1991). Cerium is retained more strongly than other REEs due to the oxidation of Ce(III) to Ce(IV) at Mn-oxide surfaces (Takahashi et al., 2000) and the precipitation of cerianite (CeO2) (Braun et al., 1990). All of the above tracers have had only limited application in the study of lateral soil development and we investigated their use in a glaciated upland catchment dominated by podzols.

In this study, we measured chemical characteristics of HPUs first developed by Bailey et al. (2014) in WS3 at both the catchment and hillslope scales. We hypothesized that Al, Fe, Mn, and C would be predictably redistributed at the hillslope scale due to lateral podzolization. Specifically, we thought that with decreasing elevation along hillslopes, Fe_o/Fe_d, Al, Mn, and spodic C would increase due to mobilization from upslope (from summits, shoulders, and backslopes) and these elements would be redistributed and would accumulate in footslope and toe-slope positions. We tested the following hypotheses: 1) in the study catchment, morphologic differences between soil types translate to distinct combinations of metal and C redistribution patterns according to dominant downslope flow direction; and 2) pedogenically significant elements and ratios (Mn_d/Fe_d, Fe_o/Fe_d, and Ce/Ce*) can be used as naturally occurring indicators of subsurface water dynamics.

2. Methods

2.1. Site description

Watershed 3 (WS3) is a hydrologic reference catchment at the Hubbard Brook Experimental Forest (HBEF) within the southern White Mountains of central New Hampshire, USA (43°56′N, 71°45′W) (Likens,

2013). Watershed 3 is 42 ha in area, with an average slope of 25%. The bedrock consists of high-grade metamorphic rocks of the Silurian Rangeley formation, but it is mostly covered by Wisconsinan basal and ablation till that varies in thickness, consistence and hydraulic conductivity, and forms the soil parent material (Bailey et al., 2014). In WS3, the till mantle is mostly derived from the Devonian Kinsman pluton, a foliated granite (Bailey et al., 2003). Dominant soil series mapped in WS3 are Becket and Skerry, which have texture classes in the fine earth fraction of fine sandy loam and sandy loam (Soil Survey Staff, 2017). These soil series are characterized by vertical permeability contrasts: moderately high to high saturated hydraulic conductivity in the mineral solum and moderately low to moderately high saturated hydraulic conductivity in the dense substratum (Soil Survey Staff, 2017). Hubbard Brook resides in the northern hardwoods ecosystem, with a mixture of deciduous and coniferous trees. Refer to Bailey et al. (2014) and Bourgault et al. (2015a) for further details.

2.2. Soils characterization

An alternative soil classification system to the traditional pedon-scale approach is hydropedologic units (HPUs), a concept that is just beginning to be utilized (D'Amore et al., 2012, 2015; Gannon et al., 2014; Tetzlaff et al., 2014; Gillin et al., 2015; Mirus, 2015; Blumstock et al., 2016). The HPU concept expands from the catena concept (Milne, 1947) by identifying functional soil zones with variations in morphology that can be directly linked to differences in hydrologic influence on soil formation (Gannon et al., 2014). Bailey et al. (2014) identified five distinct soil groups within WS3, a podzolized catchment at HBEF. Each soil group occurred in a predictable geomorphic position along hillslopes and related to inferred hydrologic conditions that were suspected due to surface and subsurface topography and position along flowpaths. Gillin et al. (2015) extended these findings by using geospatial metrics and soil morphology to map the catchment scale distribution of these five HPUs: typical podzols, E-podzols, Bhs-podzols, Bh-podzols, and bimodal podzols (Bhs and Bh horizons were distinguished by color as per Bourgault et al., 2015a). Typical podzols were the most common HPU, found on well- to moderately well-drained backslopes with predominantly vertical water movement and vertical podzolization (Gannon et al., 2014, Bourgault et al., 2015a). They had thin, discontinuous E horizons and Bhs horizons with a mean thickness of 16 cm (Bourgault et al., 2015a) overlying Bs and BC to C horizons. E-podzols and Bhs-podzols were found close together in association with shallow bedrock near the watershed divide. E-podzols had relatively thick E horizons (usually > 15 cm) and little to no underlying spodic horizon, while Bhs-podzols had little to no E horizon overlying Bhs horizons with a combined mean thickness of 39 cm (Bourgault et al., 2015a). Bh-podzols were dominated by dark-colored Bh horizons with a combined mean thickness of 37 cm (Bourgault et al., 2015a) and were found in near-stream or bench locations where lateral accumulation of water and solutes was predicted. Bimodal podzols were occasionally found in the footslope between typical and Bh-podzols. This HPU was characterized by typical podzol morphology in the upper part and an anomalous Bh horizon in the lower part, which was correlated with seasonally high water table in the lower profile (Bailey et al., 2014).

In order to further characterize the soils of WS3 and determine the redistribution of AOC, Fe, Al and Mn, 99 pedons were excavated, described, sampled, and assigned to a HPU defined as the soil functional types in Bailey et al. (2014). Of the 99 pedons sampled, 59 were collected by Bailey et al., 2014, 17 were collected by K. Harvey and S. Bailey, unpublished, and 23 were collected for this study. The soils were observed using a stratified sampling technique, with single, paired, or several sampled pedons observed along transects located purposefully to capture the range of soil variation and landforms in the catchment (Bailey et al., 2014). Each pedon was observed following excavation of a small soil pit less than 1 m^2. The soil was excavated as deeply as possible in order to observe all horizons into glacial parent material or lithic contact.

All soil horizon samples were air-dried and sieved to 2 mm to remove coarse fragments. Small subsamples were ground with agate mortar and pestle to pass through a 250 μm sieve and then extracted with citrate-dithionite (d) and acid ammonium oxalate (o) (Courchesne and Turmel, 2007). All O horizons and 1/4 of the mineral horizons were extracted in duplicate (experimental error < 10% for oxalate extracts and < 5% for dithionite extracts). Extracts were diluted by a factor of 5 and analyzed for Al_o, Fe_o, Fe_d and Mn_d using a Perkin-Elmer Optima 3000 DV Inductively Coupled Plasma – Atomic Emission Spectrometer (ICP-AES). Dithionite-extractable Al was measured but not reported due to its lack of functional definition, and as such it is not generally reported in the literature either. A representative subset of approx. 60 samples was analyzed for comparison between Al_o and Al_d (data not shown). The slope of the regression was 0.7, with $r^2 = 0.67$, meaning that dithionite extracted less Al than oxalate, and therefore the Al_d data were uninterpretable.

Optical density of oxalate extract (ODOE) was measured using a spectrophotometer at 430 nm as an index of C associated with spodic materials (Soil Survey Staff, 2004). Total organic C content was determined by dry combustion on a CE Elantech NC Soils Analyzer. Soil pH was measured with a glass electrode in 2:1 0.01 *M* $CaCl_2$ to air-dry soil (Thomas, 1986).

For 94 of the sampled pedons, Al, Fe, and Mn data for the solum (all horizons above the C horizon) in mg of an element per kg soil were summed and converted to kg of an element per m^2 using bulk density estimated from organic C content (Federer et al., 1993; Bailey et al., 2014). Spodic C was calculated for each pedon by summing and converting g kg^{-1} total organic C in all horizons below the surface (O and/or A) horizons to kg m^{-2}. Most of the data were positively skewed, so they were log-transformed before analysis to approximate a normal distribution. Univariate statistical analyses were performed in JMP Pro 9. For comparison of HPUs, one-way analysis of variance (ANOVA) with Tukey's HSD was used to compare means. Non-metric multidimensional scaling (NMS) was conducted using a Sorenson (Bray-Curtis) distance calculation on untransformed data in PC-ORD (MjM Software Design, Ver. 6). A pre-assessment of dimensionality in "Autopilot" mode was repeated twice, and then NMS was run twice (250 iterations) in order to ensure consistent results. Soil morphological variables (thickness of combined Oi/Oe/Oa, Oa, A, E, Bhs, Bs, Bh) were placed in the main matrix, and chemical parameters (Al_o, Fe_o, Fe_d, Mn_d, and spodic C) and HPU class were placed in the second matrix. These same morphological variables were also used in an NMS analysis of topographic metrics in WS3 (Bailey et al., 2014; Gillin et al., 2015) but this is the first application of the technique to study chemical distinction among the HPUs. Three odd profiles were removed from the Bh-podzols class in the final analysis because they did not group well with their assigned HPU and, upon closer look, were found to be transitional profiles in terms of both morphology and chemistry between typical podzols and Bh-podzols. Despite their near-stream location, they had thick Bhs instead of Bh horizons.

2.3. Intensive characterization of three catenas

Three catenas were sampled in WS3 (Fig. 1) at a finer scale to more thoroughly document lateral and vertical distributions of mobile elements. In this study, catenas were defined as topo-hydro-sequences (sensu Jenny, 1946) containing multiple HPUs. The catena locations were chosen to capture transitional soils between HPU end-members. Three to four pedons along each catena were described by genetic horizon. Sampling was performed by genetic horizon and in 5-cm depth increments within horizons greater than ~10 cm thick, from the soil surface through the upper 10 cm of the C horizon. Each soil sample was analyzed as previously described. In order to provide further information about pedogenic and redox processes, rare earth elements (including La, Ce, and Pr reported herein) were quantified in the oxalate

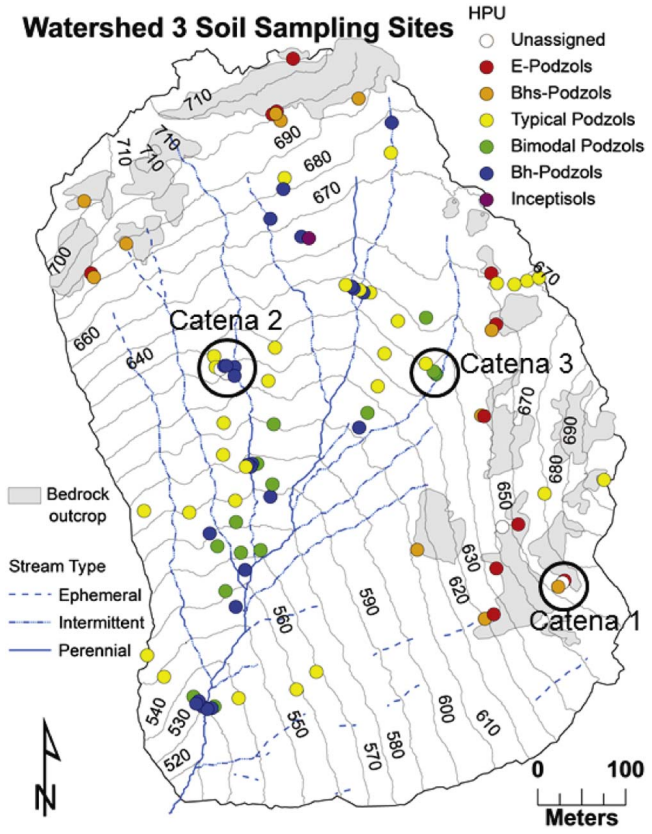

Fig. 1. Map of watershed 3 at Hubbard Brook experimental forest, produced in ArcGIS 10.0, showing soil sampling locations, hydropedologic unit designations, bedrock outcrops, and streams/ stream types. Also shown are locations of Catenas 1, 2, and 3 (see Fig. 3). Contours show elevation in m. "Unassigned" refers to transitional soil profiles that did not fit the central concept of any HPU. A few of these were removed from multivariate analysis due to outlier status. The watershed boundary and stream channels were generated in ArcGIS 10.1 by Gillin et al. (2015) from a 1 m DEM derived from a LiDAR dataset collected by Photo Science, Inc. in April 2012 for the White Mountain National Forest. Stream channels determined by ArcGIS (based on assumption of minimum upslope accumulated area to generate surface flow) were modified based on GPS mapping of channels observed in the field. Bedrock outcrop polygons were also generated by Gillin et al. (2015) using a field survey combined with LiDAR imagery.

extracts using a Perkin Elmer Elan 6000 quad inductively coupled plasma – mass spectrometer (ICP-MS). Concentrations were determined based on calibrations constructed using ten digested international rock standards diluted to have REE concentrations spanning the range observed in these soil extracts. Thallium was used as the internal reference standard, and concentration values were precise to better than 3% based on comparison of replicate measurements performed on a subset of the samples. Cerium anomalies were described using Ce/Ce*, which is the ratio of the concentration of observed Ce divided by predicted Ce. Predicted concentration of Ce, denoted as Ce*, was calculated as an average of normalized concentrations of the neighboring REEs La and Pr. Rare earth element concentrations were normalized by dividing by average total REE content of six deep till samples (141–218 cm) from WS3 that were assumed to be close to unweathered parent material (Burns, 2012). Although the average Ce/Ce* for these six deep till samples is 1.0 relative to traditional normalizing schemes (e.g., chondrites, shale averages), values range from 0.82 to 1.14 thus Ce/Ce* values of oxalate extracts reported here have a reasonable uncertainty of +/− 15%.

3. Results

3.1. Catchment-scale distribution of AOC and metals

Clear grouping of pedons by the five HPUs was observed using non-metric multidimensional scaling (NMS) of horizon thicknesses and chemical composition (Fig. 2). Pre-assessment of data suggested that the ideal number of dimensions was three. This result minimized both stress (which was 11.16 for the 3-axis ordination) and the number of interpretable axes. Axis 1 corresponded to spodic C, Axis 2 corresponded to Fe_o, and Axis 3 corresponded to Mn_d. Of the two-dimensional projections, Axes 2 (Fe_o) and 3 (Mn_d) showed the best separation of HPUs (Fig. 2b). Dithionite-extractable Mn was not correlated with Al_o, Fe_o, Fe_d, or spodic C.

Soils classified as typical podzols had intermediate-sized contents of extractable Fe, Al, Mn, and organic C (Table 1, Fig. 2). These soils had smaller pools of Fe_d, Mn_d, and spodic C than the Bhs- and Bh-podzols (Table 1, Fig. 2), but larger content of those elements than E-podzols. The E-podzols had thick E horizons and near absence of spodic materials, and the lowest quantities of Al, Fe, and spodic C (Table 1, Fig. 2). Bhs-Podzols contained much higher Al, Fe, and spodic C compared to E-podzols (Table 1, Fig. 2). Overall, Mn_d concentrations were relatively high in soils observed on the west side of the catchment and relatively low in all soils observed on the east side of the catchment (Supp. Fig. 1). Bh-podzols had similarly sized extractable Fe pools compared to the other HPUs, not including E-podzols (Table 1). However, Bh-podzols contained significantly higher quantities of Mn_d compared to the other HPUs (Table 1, Fig. 2). Bhs-podzols and bimodal podzols were similar in terms of chemical composition (Table 1, Fig. 2). Al_o was higher in Bhs-podzols, Bh-podzols, and bimodal podzols relative to typical podzols, but the effect was not significant due to large variation (Table 1). Spodic C contents were highest in Bhs-podzols, Bh-podzols, and bimodal podzols relative to typical and E-podzols (Table 1, Fig. 2, Supp. Fig. 2). Actual concentrations of Fe_o, Fe_d, Mn_d, Al_o, organic C and spodic C by horizon type were reported in Bourgault et al. (2015a).

The Fe active ratio, Fe_o/Fe_d, had little variability in WS3 related to topographic position or HPU classification (Supp. Fig. 3). Low Fe_o/Fe_d values (~0.4) were observed for E and C horizons, while high Fe_o/Fe_d values (~0.8) were observed for spodic horizons. The ratio of Mn_d/Fe_d also did not vary with topographic position or HPU; instead, Mn_d/Fe_d was highest in the soil surface and decreased with depth (Supp. Fig. 3).

3.2. Intensive hillslope scale studies: soil composition

Three catenas were sampled to investigate lateral transfer between specific HPU combinations. Groundwater monitoring wells were used to confirm the hydrologic character of each HPU (Supplementary Material). Catena 1 (Figs. 1 and 3) represented an E- to Bhs-podzol transition near the top of the catchment. Each of the two HPU end-member pedons was observed, as well as one transitional pedon in between them. The majority of the E-podzol (pedon 1.1) was leached of Al, Fe, spodic C, Ce_o, and La_o, except in the thin Bhs horizon (Table 2, Fig. 4, Supp. Table 1). Dithionite- and oxalate-extractable Fe in the transitional pedon (1.2) showed no pattern, but Al_o, Ce_o, and La_o showed a consistent increase with depth (Fig. 4). The Bhs-podzol (pedon 1.3) showed distinct maxima of Al_o, Fe_o, Ce_o, and La_o in the middle of the spodic horizon (Fig. 4, Supp. Table 1). Overall, in Catena 1, amounts of Al_o, Fe_o, spodic C and Ce_o increased with decreasing elevation, while Fe_d generally increased and Mn_d was low throughout (Table 2).

Catena 2 (Figs. 1 and 3) represented a typical podzol to Bh-podzol transition. It consisted of a typical podzol end-member on a steep backslope (pedon 2.1), and a Bh-podzol end-member in a gently sloping near-stream zone (pedon 2.4), with two transitional soil profiles in

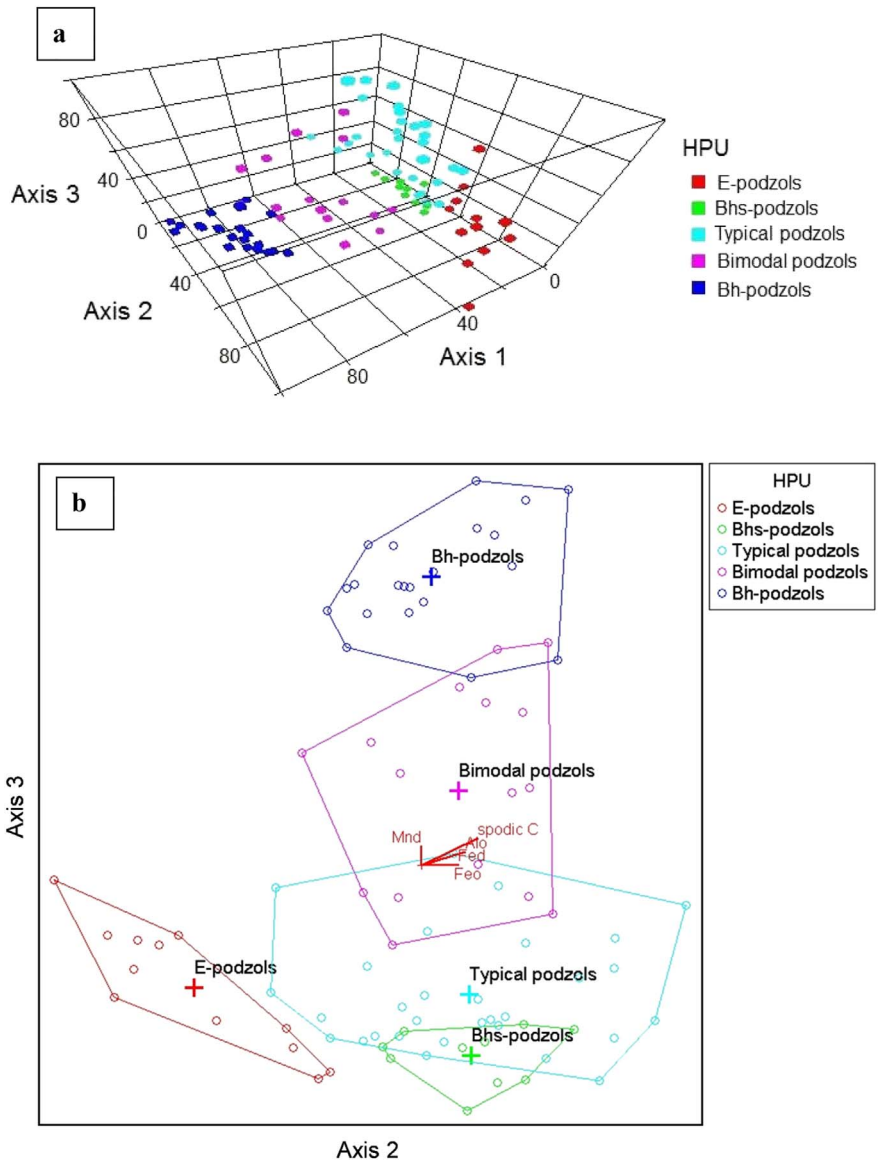

Fig. 2. Non-metric multidimensional scaling of HPUs using horizon type thicknesses; a) 3-D projection; b) 2-D projection along axes showing best separation of groups. Length of vector indicates relative strength of correlation. Axis 2 corresponded with Fe_o and Axis 3 corresponded with Mn_d.

between (pedons 2.2 and 2.3). In general, pools of Fe_o, Fe_d, Mn_d, spodic C, and Ce_o increased towards the stream from pedons 2.1 to 2.3, and spodic C and Ce_o continued to increase in pedon 2.4, but Fe_o, Fe_d, and Mn_d decreased slightly (Table 2). Oxalate-extractable Al did not show a predictable trend with decreasing elevation (Table 2). Of the four profiles in catena 2, pedon 2.1 had the smallest pools of all measured elements (Table 2) and had the thinnest spodic horizon (Supp. Table 1). The extraction data for pedon 2.2 showed two distinct maxima of Fe_d, Fe_o and Al_o: the first and largest maxima occurred in the Bhs horizon, and lesser maxima occurred in the middle of the BC horizon (Fig. 5a-b and d). Pedon 2.3, a Bh-podzol in a footslope, showed a greater thickness (depth interval) of accumulation of high concentrations of Fe_o and Al_o than pedons 2.1 and 2.2 (Fig. 5b and d), and had the largest pool of Mn_d in Catena 2 (Table 2). Pedon 2.4, the Bh-podzol end-member, also had a great thickness (depth interval) of accumulation of Fe_d, Fe_o and Al_o, and an increase in Mn_d similar to pedon 2.3, but with higher Fe_d, Fe_o and Al_o maxima and a lower Mn_d maximum than pedon 2.3 (Fig. 5). This Bh-podzol showed a very prominent spike in concentrations of Ce_o and La_o that coincided with the Al_o maximum in the Bh1 horizon at approx. 40 cm (Fig. 5d, e and g).

Catena 3 (Figs. 1 and 3) represented a typical to bimodal sequence

Table 1
Soil profile totals of oxalate-extractable (o) and dithionite-extractable (d) secondary metal concentrations, total organic C, and spodic C (total organic C below O and/or A horizons) by hydropedologic unit (HPU). Means ± standard error are reported. Means in each column with the same letter are not significantly different (α = 0.05).

HPU	n	Al_o	Fe_o	Fe_d	Mn_d	Total organic C	Spodic C
		kg m^{-2}					
E-podzols	12	0.83 ± 0.67^{b}	1.39 ± 0.69^{b}	2.03 ± 0.84^{c}	0.10 ± 0.05^{bc}	18 ± 2^{b}	5 ± 2^{c}
Bhs-podzols	11	4.19 ± 0.70^{a}	5.87 ± 0.72^{a}	7.21 ± 0.88^{ab}	0.22 ± 0.05^{ab}	29 ± 2^{a}	22 ± 2^{a}
Typical podzols	30	2.89 ± 0.42^{a}	3.24 ± 0.43^{a}	4.08 ± 0.53^{b}	0.02 ± 0.03^{c}	18 ± 1^{b}	12 ± 1^{b}
Bimodal podzols	15	4.09 ± 0.60^{a}	4.25 ± 0.61^{a}	6.48 ± 0.75^{a}	0.05 ± 0.04^{abc}	29 ± 2^{a}	22 ± 2^{a}
Bh-podzols	25	4.04 ± 0.47^{a}	3.79 ± 0.48^{a}	5.15 ± 0.58^{ab}	0.18 ± 0.03^{a}	24 ± 2^{a}	18 ± 1^{a}

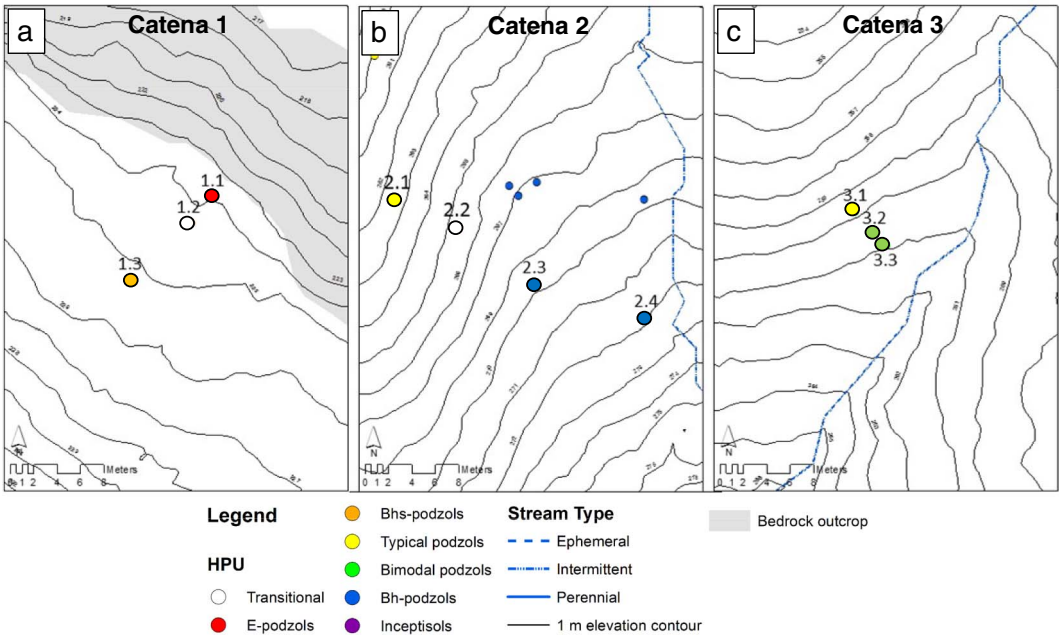

Fig. 3. Maps showing (a) catena 1; (b) catena 2; and (c) catena 3. See Fig. 1 for locations in Watershed 3. Contour lines show elevation in m.

near a stream channel. The typical podzol (3.1) had very high quantities of Fe_d, Fe_o and Al_o (Table 2), but the depth profile showed a bimodal distribution not observed in the morphological description (Fig. 6a, b, and d; Supp. Table 1). Concentrations of Fe_d, Fe_o and Al_o peaked in the Bhs horizon, then decreased in the Bs1 horizon, but increased again in the Bs2 horizon (Fig. 6a, b, and d; Supp. Table 1). Oxalate-extractable Ce and La generally increased with depth in pedon 3.1 (Fig. 6e and g). Two bimodal podzols were observed several m downslope of pedon 3.1. Pedon 3.2 had maximum concentrations of Al_o, Ce_o, and La_o that coincided with the top of the Bh horizon at 68 cm (Fig. 6d, e, and g; Supp. Table 1). Dithionite- and oxalate-extractable Fe peaked in the Bhs horizon at 32 cm, and there were lesser maxima of Fe_d and Fe_o and another Al_o peak that coincided with the top of the Bh horizon at 68 cm (Fig. 6a, b, and d; Supp. Table 1). Pedon 3.3 had a mixed Bhs/Bh horizon that had a spike in concentrations of Fe_o, Al_o, Ce_o, and La_o at approx. 40–60 cm (Fig. 6).

Positive Ce-anomalies were found in the lower part of all soil profiles from all three catenas except for the E-podzol and the transitional soil just below it (pedons 1.1 and 1.2). The magnitude of Ce/Ce* also increased downslope in all three catenas (Figs. 4h, 5h, and 6h). The only exception to this observation was pedon 2.1 (typical podzol); however, the actual quantity of Ce_o was lower in pedon 2.1 than in the three other pedons downslope in Catena 2 (Table 2, Fig. 5e). Total pools of Ce_o increased two- to threefold in the downslope direction for all three catenas (Table 2). Pedon 2.4, a Bh-podzol, showed a spike in Ce/Ce* (and Ce_o, La_o, and Fe_o) in the upper Bh1 horizon at 30 cm (Fig. 5; Supp. Table 1). Pedon 3.2, a bimodal podzol, showed a similar spike in Ce/Ce* in the Bhs1 horizon at 30 cm (Fig. 6h, Supp. Table 1).

4. Discussion

4.1. Genesis of hydropedologic units

In humid climates, podzolization tends to occur in well- to moderately well-drained conditions with the assumption of predominantly unsaturated vertical water flux (Feldman et al., 1991; Freeland and Evans, 1993; Li et al., 1998; Melkerud et al., 2000). A notable exception to this assumption is podzols developed in climates warmer than that of Hubbard Brook, where persistent, fluctuating water tables produce characteristic morphology and removal of secondary Fe (Tan et al., 1999; Harris and Hollien, 2000; Buurman et al., 2013a,b). Typical podzols of WS3 such as pedon 2.1 experience the former conditions, evidenced by drainage class, lack of water table in the solum, and measurements of unsaturated soil water potential confirming vertical water flux in the unsaturated zone (Supp. Fig. 4b; Bailey et al., 2014; Gannon et al., 2014, 2017). Therefore, genesis of this HPU is consistent with classical descriptions of podzolization summarized in McKeague

Table 2
Soil profile totals for dithionite-extractable (d) and oxalate extractable (o) secondary metals and cerium (Ce), and spodic C (total organic C below the O and/or A horizons).

Catena no.	Relative position in catena	Pedon ID	HPU	Fe_d	Mn_d	Al_o	Fe_o	Spodic C	Ce_o
				kg m^{-2}					
1	Upslope	1.1	E-Podzol	1.29	0.01	0.42	0.30	4	1.1×10^{-3}
	↓	1.2	Transitional	4.42	0.01	1.10	2.51	9	1.8×10^{-3}
	Downslope	1.3	Bhs-Podzol	3.56	0.01	1.65	2.20	12	2.5×10^{-3}
2	Upslope	2.1	Typical Podzol	5.84	0.06	7.55	4.69	20	3.0×10^{-3}
	↓	2.2	Transitional	9.57	0.13	9.83	7.15	20	5.8×10^{-3}
		2.3	Transitional	10.36	0.34	8.96	7.89	29	4.9×10^{-3}
	Downslope	2.4	Bh-Podzol	7.30	0.16	7.97	5.51	26	9.4×10^{-3}
3	Upslope	3.1	Typical Podzol	8.46	0.03	11.44	6.73	27	2.6×10^{-3}
	↓	3.2	Bimodal Podzol	5.27	0.01	4.56	4.25	21	6.8×10^{-3}
	Downslope	3.3	Bimodal Podzol	5.38	0.01	3.13	3.80	16	6.8×10^{-3}

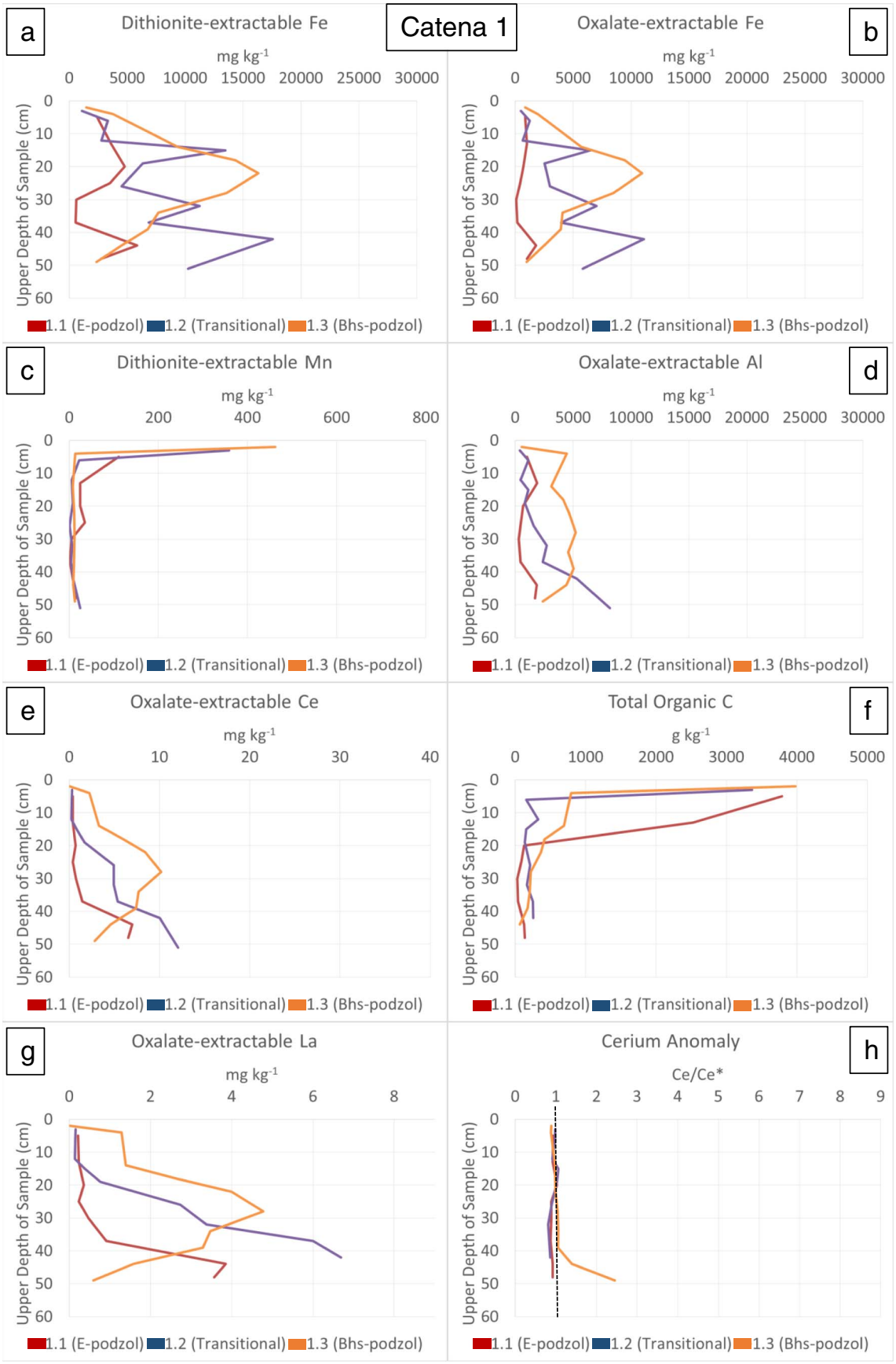

Fig. 4. Soil depth profiles of extractable metals, organic carbon, REEs, and Ce anomalies for Catena 1. Soil profiles were sampled in 5-cm increments within each horizon.

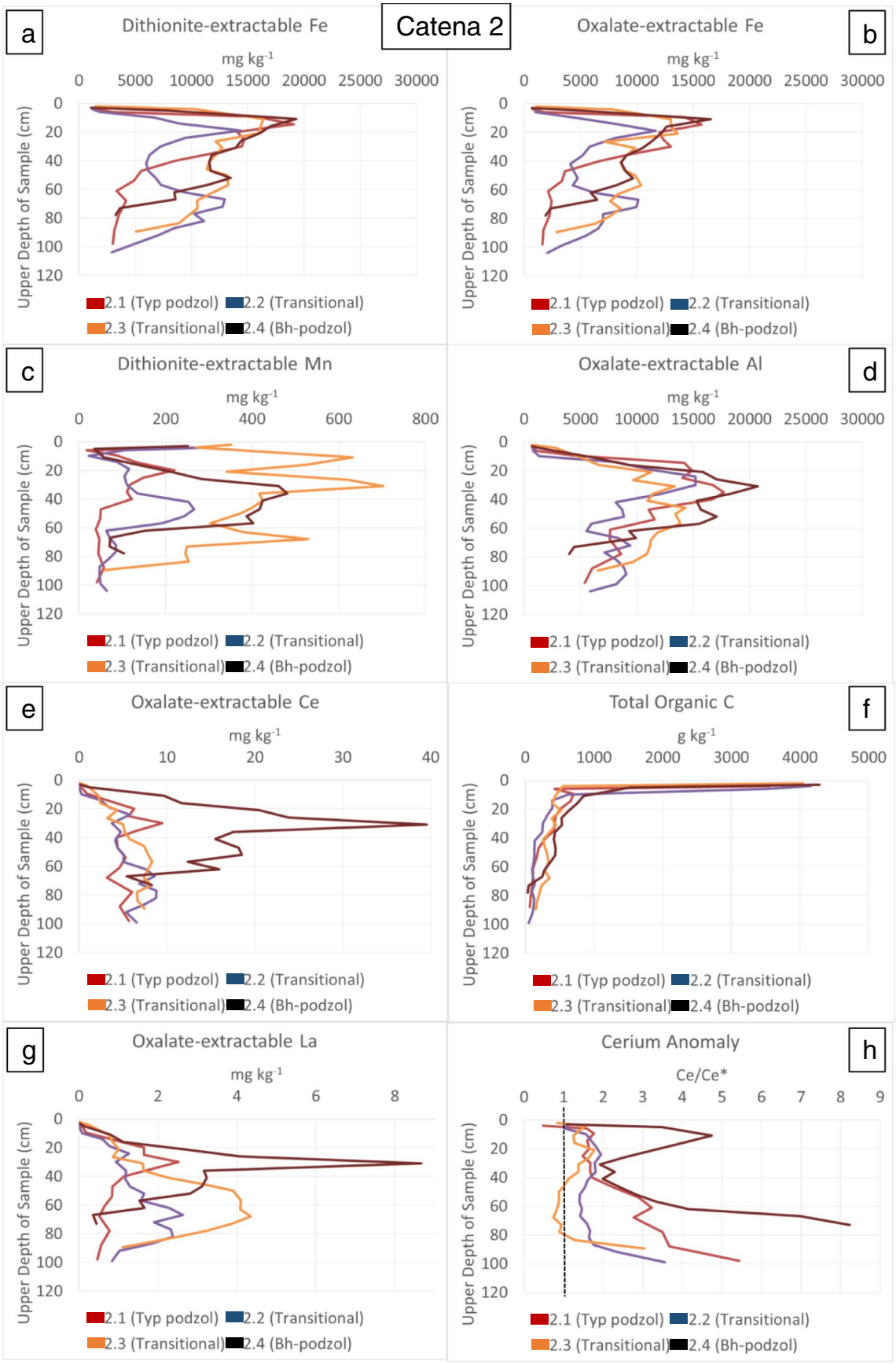

Fig. 5. Soil depth profiles of extractable metals, organic carbon, REEs, and Ce anomalies for Catena 2. Soil profiles were sampled in 5-cm increments within each horizon.

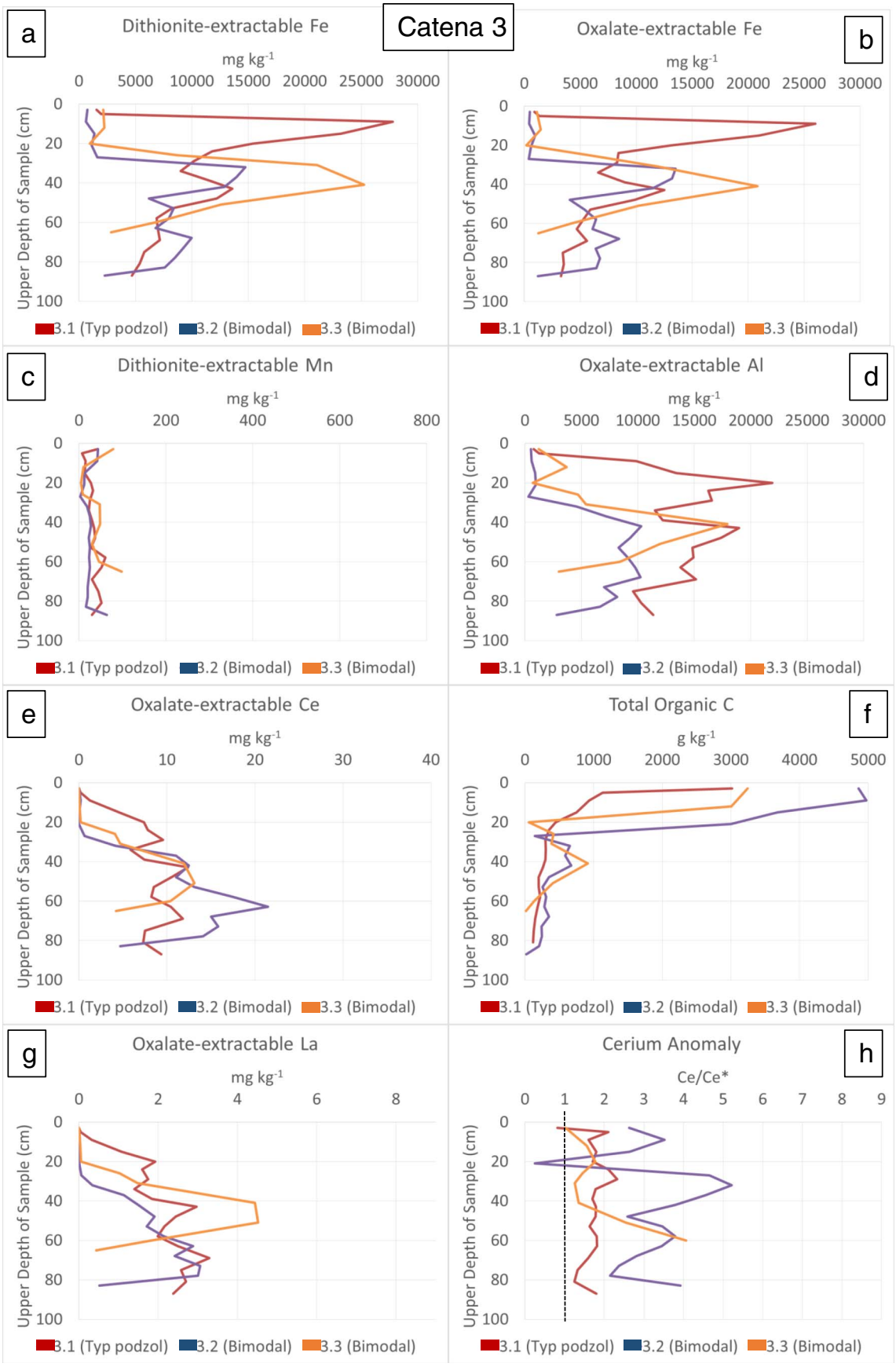

Fig. 6. Soil depth profiles of extractable metals, organic carbon, REEs, and Ce anomalies for Catena 3. Soil profiles were sampled in 5-cm increments within each horizon.

et al. (1983) and Lundstrom et al. (2000). The chemical composition of typical podzols was also consistent with vertical podzolization under unsaturated conditions. Depth and thickness of the spodic horizon is thought to be determined by the vertical distance that soluble amorphous organometallic complexes (AOC) can translocate with downward-percolating water before reaching saturation and precipitating from soil solution, which is related to pH as well as C/sesquioxide ratios (Buurman, 1985).

Aside from typical podzols, the soils of WS3 experience seasonally fluctuating groundwater conditions with episodic saturation, sometimes lasting only hours, and drainage of the solum on an event basis (Bailey et al., 2014: Gannon et al., 2014). These conditions are considered drier than wetter podzols of coastal plains (see Section 4.5), with moderately well to somewhat poorly drained soils prevalent in WS3 in the lowest slope positions. Bh-podzols such as pedon 2.4 had the most persistent water table of the HPUs, characterized by the presence of a water table up to 70% of the time in Bh horizons; however, the top of the Bh horizon often occurred above the seasonally high water table (Bailey et al., 2014; Gannon et al., 2014). It is likely that pedon 2.4 had a water table regime similar to other Bh-podzols in WS3, where the lower part of the solum (lower Bh horizons) would have been nearly always saturated, and the upper part of the solum would have experienced brief, episodic saturation following storm events (Gannon et al., 2014). This variation in groundwater height in a steep catchment was the driver of lateral soil development in all but the typical podzols.

4.2. Chemical composition of hydropedologic units

At the catchment scale, the five HPUs (typical podzols, Bh-podzols, bimodal podzols, E-podzols, and Bhs-podzols) were chemically distinct from one another. There was at least one pairwise difference among the HPUs with respect to pools of each measured variable associated with podzolization: Al_o, Fe_o, Fe_d, Mn_d, total organic C, and spodic C (subsurface organic C) (Table 1). Functional classification of WS3 soils using the HPU scheme developed by Bailey et al. (2014) therefore appeared to group soil profiles according to differences in chemical composition as well as horizon type and thickness. In general, soils with thicker spodic horizons had larger pools of extractable metals and subsoil organic C.

Typical podzols tended to have spodic horizons that were relatively thin, but had higher concentrations of metals and C per mass compared to other HPUs (Bourgault et al., 2015a). The resulting pools of metals and C in typical podzol profiles in WS3 were generally intermediate among the HPUs (Table 1) and consistent with other non-hydric podzols in humid temperate regions (Blume and Schwertmann, 1969; Barrett, 1997). Bh-podzols associated with slope breaks and near-stream topography (Gillin et al., 2015) were distinct from the other HPUs in that they tended to have larger pools of Mn_d and organic C (both total and spodic C) (Table 1), reflective of their thick, dark spodic horizons (Supp. Table 1). Bhs-podzols and bimodal podzols were similar in terms of chemical composition, with larger quantities of secondary Fe and spodic C in the profile compared to typical podzols (Table 1, Fig. 2). This was not unexpected given that they had similarly thick, laterally developed spodic horizons (Bourgault et al., 2015a), including Bhs horizons in both (Supp. Table 1).

Characterizing chemical differences between HPUs is essential for understanding spatial pattern of solute sources in a headwater catchment. For example, D'Amore et al. (2015) characterized dissolved organic carbon (DOC) output from several different HPUs in Alaska, USA. The authors were thus able to use HPUs as an effective predictor of catchment DOC export and regional DOC flux. A similar approach was used in WS3 at HBEF using the current HPU classification. In that study, elevated DOC at the catchment outlet was observed when water table was measured in HPUs with high observed DOC in soil and groundwater (Gannon et al., 2015).

4.3. Lateral podzolization downslope of bedrock exposure

In WS3, E- and Bhs-podzols were always found within several meters of each other and experienced lateral flow following storm events, evidenced by brief, episodic saturation with groundwater sourced from nearby rock outcrops and perched by shallow underlying bedrock (Bailey et al., 2014; Gannon et al., 2014). This episodic lateral water movement over shallow bedrock resulted in E-podzols with thick, bleached E horizons and near absence of underlying spodic materials (Table 1, Fig. 2, Supp. Table 1). Bhs-podzols appeared to be the site of lateral deposition of spodic materials eluviated from these E-podzols. As a result, Bhs-podzols contained much larger pools of Fe_d, Fe_o, Al_o, and spodic C compared to E-podzols (Table 1, Fig. 2). Others have documented podzols with similar morphology and chemistry in Europe. Sommer et al. (2001) described two distinct podzol types assumed to be the result of lateral podzolization: “E-Spodosols” had thick E horizons, thin spodic horizons, and were leached of extractable Al, Fe, Mn, and organic C throughout most of the soil profile. On the other hand, “Bs-Spodosols” had thin E horizons and thick spodic horizons that contained much larger pools of those elements.

4.4. Lateral podzolization at slope breaks and near streams

In near-stream zones or bench areas where Bh-podzols were found, spodic materials were thought to accumulate in the subsurface due to a decrease in slope, which reduced hydraulic gradients and altered downslope drainage conditions (e.g., Crave and Gascuel-Odoux, 1997; Hjerdt et al., 2004). Previous studies had hypothesized that the Bh horizon in WS3 was mostly developed through lateral podzolization (Bailey et al., 2014; Bourgault et al., 2015a; Gannon et al., 2017). This hypothesis was supported by the observation that the top of the Bh horizon extended above the water table and slope-parallel unsaturated water flux was observed in the upper Bh horizon (Gannon et al., 2017). Therefore, it was concluded that the lower, frequently saturated part of the Bh horizon contained an accumulation of spodic materials deposited laterally by groundwater, while the upper, predominantly unsaturated part of the Bh horizon in Bh-podzols contained spodic materials deposited by slope-parallel unsaturated flow (Gannon et al., 2017). The morphology, micromorphology, and chemical composition of Bh horizons further supported the hypothesis of the lateral mode of podzolization (Bailey et al., 2014; Bourgault et al., 2015a). The high Mn_d content of Bh-podzols at the catchment scale (Table 1) was likely due to lateral translocation and deposition of this element. Catena 2 showed this pattern of redistribution of Mn at the hillslope scale. Pedons 2.3 and 2.4, both Bh-podzols, showed greater concentrations of Mn_d over a greater depth interval than pedons 2.1 and 2.2, both typical podzols (Fig. 5c). There are multiple possible mechanisms to explain this phenomenon. First, it is possible, though unlikely due to Mn chemistry, that Mn may be directly involved in podzolization. In this case, Mn would be complexed with organic matter and transported in a soluble or colloidal AOC. However, the lack of correlation between Mn and elements involved directly in podzolization does not support this explanation (Fig. 2). A more likely explanation for accumulation of Mn in Bh-podzols is related to Mn redox activity and lateral flowpaths. Insoluble Mn(III, IV) can easily become mobile in acid soils due to reductive dissolution to soluble Mn(II). It is possible that Mn(II) becomes translocated downslope with lateral flow paths and then becomes oxidized/precipitates on surfaces of existing Mn oxides, Fe oxides, or AOC in lower slope positions, where Bh-podzols are formed. Divalent Mn may also become oxidized by microbes (Tebo et al., 2005). Others have documented increasing Mn_d content with decreasing elevation along hillslopes and in convergent topographic settings; however, these studies did not determine Mn oxidation state (McDaniel et al., 1992; Park and Burt, 2002). Bh-podzols also had significantly larger pools of spodic C (Table 1), possibly accumulated through lateral podzolization and/or fluctuating water table. Jankowski (2014) described “accumulative”

podzols in closed depressions with relatively thick Bhs horizons and larger pools of Al_o and Fe_o that were thought to be developed via lateral podzolization from surrounding hillslopes composed of soils with thinner spodic horizons and smaller pools of Al_o and Fe_o. The presence of soils with thick spodic horizons and large pools of extractable Al, Fe, Mn and C immediately adjacent to soils mostly leached of these elements illustrates the potential for large differences in soil and ecosystem function within just a few m along hillslopes in which lateral podzolization has occurred.

Bimodal podzols were relatively rare in WS3, and their spatial distribution could not be modeled accurately (Gillin et al., 2015). Nonetheless, the morphology of these soils suggested both vertical and lateral development; therefore, they were thought to be important to the objectives of the study. Pedon 3.1 was classified as a typical podzol and showed horizonation consistent with vertical podzolization (Supp. Table 1). Pedon 3.1 showed near absence of water table in the solum (Supp. Fig. 4c), which was expected based on water table dynamics of other typical podzols (Gannon et al., 2014). However, the extraction chemistry for pedon 3.1 revealed bimodal profile distributions of Fe_d, Fe_o and Al_o (Fig. 6a, b, and d). The first maxima occurred between 10–20 cm in the Bhs horizons and there were lesser Fe and Al maxima at 43 cm in the Bs2 horizon (Fig. 6a, b, and d; Supp. Table 1). These patterns were not characteristic of a typical podzol, but could be due to preferential flow paths and/or unsaturated lateral flow. Pedons 3.2 and 3.3 showed morphology characteristic of bimodal podzols (Supp. Table 1) and the monitored pedon 3.3 showed water table dynamics characteristic of bimodal podzols (Supp. Fig. 4c; Gannon et al., 2014). Following summer storm events, the water table would rise to 20–30 cm for a few days and then drop to its usual level at 40–50 cm (Supp. Fig. 4c). In pedon 3.3, the association of spodic materials with water table in this zone was apparent. The spike in concentrations of Fe and Al at 43 cm (Fig. 6a, b, and d) may be attributed to lateral deposition of spodic materials in the zone saturated by laterally flowing groundwater, or fluctuating water table causing dissolution/re-precipitation of AOC. The chemistry, morphology, and water table dynamics of soils observed at slope breaks and near streams support our hypothesis that lateral podzolization is dominating soil-forming processes and is redistributing specific elements in these areas. The sequestration of Al, Fe, Mn, and organic C in bimodal and Bh-podzols due to lateral podzolization highlights the importance of these soils in biogeochemical cycling of these elements. As they tend to be associated with the stream network (Gillin et al., 2015), they likely serve as controls on headwater stream chemistry and may explain gradients in metal concentrations in the streams (Zimmer et al., 2012). In addition, the lateral accumulation of organometallic complexes suggests the complexity of the podzolization process at the hillslope/ landscape scales and poses challenges to soil classification systems based on pedon-scale genesis and morphology.

4.5. Comparison of Hubbard Brook podzols with wetter podzols of coastal plains

Podzols develop in a variety of hydrologic and temperature regimes. In the literature, there are multiple studies of podzols formed in coastal plain regions such as the eastern US and southeastern Brazil, but these soils contrast with those of HBEF. In coastal plain regions, the climates are warmer than that of HBEF, and podzols usually form in sandy marine sediments under conditions of seasonal saturation and reduction associated with fluctuating, persistent water tables in nearly level landscapes with very low topographic and hydrologic gradients (Harris, 2001; Buurman et al., 2013a,b). These wet podzols (conceptualized as Alaquods in USDA Soil Taxonomy) are sometimes hydric due to shallow saturation with groundwater, are dominated by amorphous Al-OM compounds, and have very little secondary Fe due to reductive dissolution of Fe oxides (Kuehl et al., 1997; Buurman et al., 2013a,b; Stolt et al., 2016). In many cases of these wet podzols, amorphous Al is thought to complex with organic acids and precipitate in spodic horizons associated with seasonally high water table (Tan et al., 1999; Harris and Hollien, 2000, Stolt et al., 2016). In addition, saturated lateral flow of groundwater produces transport and accumulation of AOC in horizons with sharp boundaries, producing dramatic differences in soil morphology across catenas with pronounced differences in drainage (Buurman and Vidal-Torrado, 2015). However, we argue that this is not the same process forming podzols at HBEF due to the prevalence of lateral unsaturated flow, transient water tables, and subtle differences in drainage (Bourgault et al., 2015b). The presence of seasonally high water table in the Bhs- and Bh-podzols of WS3 may suggest the development of reducing conditions in these soils and similarity to wet podzols of coastal plains. The presence of seasonally high water tables and lateral podzolization may also lead one to compare HBEF podzols with those previously described in the literature in wetter catenas with more persistent water tables and removal of secondary Fe (Buurman and Vidal-Torrado, 2015). However, the development of Bhs- and Bh-podzols in WS3 appears to contrast with that of wetter coastal plain podzols because Bhs- and Bh-podzols do not appear to be dominated by reducing conditions and persistent, regional water tables. Unlike wetter podzols of coastal plain regions, Bhs- and Bh-podzols in WS3 had abundant secondary Fe (Table 1); for example, peak Fe_o and Fe_d concentrations were 10,000 and 15,000 mg kg^{-1} respectively in pedon 1.3 (Fig. 4a-b). In pedon 1.3, water table often rose between 0–30 cm during the growing season (Supp. Fig. 4a), but it is likely that oxidizing conditions persisted in the upper spodic horizon because the water table was only sporadically present and did not stay long enough to cause reducing conditions in this zone. The time required to develop the reducing conditions necessary to form redox features depends on activity of Fe-reducing microbes, which varies with temperature and organic C levels. Typically, soil must be fully saturated for days to weeks during the growing season under ideal conditions for redox features to form (Vepraskas, 2001). In pedon 1.3, below 30 cm, where the lower Bhs horizon was nearly always saturated, conditions also appeared to be mostly oxidizing due to the high amounts of Fe (Fig. 4a-b), absence of visible Fe depletions, and presence of only few, faint Fe concentrations in the lowest Bhs horizon (Supp. Table 1). In the shallow-to-bedrock areas such as Catena 1, it is possible that rapid lateral flow from the shallow-to-bedrock areas may have provided oxygenated water downslope, preventing it from becoming anaerobic. Stagnant water is required to form reducing conditions, as moving water tends to bring O_2 into the soil (Cogger and Kennedy, 1992).

The distribution of elements within the whole catchment further supports our hypothesis that the development of wetter podzols in WS3 contrasts with development of wetter podzols of the coastal plains. Bh-podzols did not have significantly different Fe_d, Fe_o or Al_o pools compared to typical podzols (Table 1). However, the actual concentrations of secondary Fe were lower in Bh horizons relative to Bhs horizons of typical podzols upslope; this difference in secondary Fe concentration was possibly due to dispersal of AOC over a greater volume with lateral transport by water (Bourgault et al., 2015a). Decreasing secondary Fe concentration in Bh horizons with decreasing elevation was also observed by Fritsch et al. (2009), who suggested the pool of Fe oxides was depleted through precipitation upslope and/or biomineralization of AOC under wetter conditions that allowed export of reduced Fe(II) from the Bh horizon. Catena 2, however, did not show any obvious downslope trends in secondary Fe pools or concentrations (Table 2; Fig. 5a-b).

Podzols that are mostly devoid of Fe are problematic for classification and hydric soil determination due to the lack of expression of redoximorphic features (Kuehl et al., 1997; Stolt et al., 2016). The soils of WS3 should not have this problem due to their abundant amounts of secondary Fe; therefore, if they were indeed hydric, there would likely be redoximorphic features as evidence of reducing conditions in the upper profile. The soils in WS3 support upland vegetation, are relatively coarse textured (fine sandy loam to sandy loam; Bailey et al., 2014),

highly transmissive and occur along relatively steep slopes. These are not poorly drained and do not have conditions of saturation long enough during the growing season to develop reducing conditions in the upper part; however, these soils show predictable variation in hydrological flow paths and development and are distinctly different from wetter podzols of coastal plain regions described in the literature.

4.6. Applicability of hydropedologic tracers

Other authors have shown that redistribution of Fe via lateral flow and reduction/oxidation leads to higher Fe_o/Fe_d downslope, including podzols (Park and Burt, 1999, 2002). However, in WS3 the Fe_o/Fe_d appeared to be determined solely by podzolization, and there were no downslope trends. High Fe_o/Fe_d was only associated with spodic horizons (Supp. Fig. 3), where complexation of Fe with organic matter prohibited crystallization of Fe oxides. The depth profiles of Fe_o/Fe_d were very similar to those of Michigan (USA) podzols analyzed by Barrett (1997). There was a strong correlation between Fe_o and Fe_d ($r = 0.94$), and there was, on average, approximately 20% more Fe_d present than Fe_o for all soil samples. This consistent and low percentage increase of Fe_d over Fe_o suggests that most or all of the secondary Fe in WS3 was found as poorly crystalline oxides or organically complexed forms, and that the dithionite reagent was probably extracting more of the same pool of Fe than the oxalate extraction, rather than dissolving a separate fraction of well-crystalline minerals not dissolved by the oxalate reagent.

Manganese appeared to be quite mobile in WS3 because it was accumulating in near-stream and bench zones in Bh-podzols (Table 2; Fig. 2; Supp. Fig. 1). The complexation ability of Mn in its various oxidation states with soil organic matter is not well understood. Some have suggested that Mn is directly involved in podzolization (Blume and Schwertmann, 1969), but other factors may be more important in determining Mn distributions in WS3. Dithionite-extractable Mn concentrations tended to be highest in the surface (O and/or A) horizons, and in catenas with relatively higher quantities of Mn_d, it also increased in B horizons downslope. The utility of a hydropedologic tracer would depend on starting with an even distribution in the parent material. However, Mn_d was not evenly distributed throughout WS3 (Supp. Fig. 1). Of the three catenas (Figs. 4c, 5c, and 6c), the concentrations of Mn_d were highest in Catena 2 (Fig. 5c). These concentrations were characteristic of other soils on the west side of the catchment, which tended to have higher Mn_d concentrations than those on the east side (Supp. Fig. 1), perhaps due to input of Mn from high-Mn seeps found only on the west side (Bourgault, 2014).

Observations of positive Ce anomalies in WS3 (Figs. 4h, 5h, and 6h) suggest that the presence and vertical distribution of positive Ce anomalies may be diagnostic of lateral flow and depth to seasonally high water table, and may be a better indicator than Fe_o/Fe_d and Mn_d/Fe_d (Supp. Fig. 3). For all three catenas, the amount of Ce per area increased with decreasing elevation (Table 2), and Ce anomalies generally increased downslope as well, indicative of the overall redistribution of Ce with lateral flowpaths and preferential sorption of Ce relative to other REEs. However, the depth distribution of positive Ce anomalies at the pedon scale provides the strongest connection to lateral flow and depth to seasonally high water table along catenas. For example, in zones of the catchment with E- and Bhs-podzols developed under lateral flow conditions (e.g., Catena 1), REEs mobilized from weathering of primary minerals are leached congruently from E-podzols resulting in solutions having no Ce-anomaly ($Ce/Ce^* \sim 1$; Fig. 4h). REE-bearing accessory minerals such as monazite $(Ce,La)PO_4$ and allanite $((Ce,Ca,Y,La)_2(Al,Fe^{3+})_3(SiO_4)_3(OH))$ are common in igneous and metamorphic rocks such as those comprising Hubbard Brook bedrock and glacial drift. Cerium(III) then deposits preferentially with respect to the other REEs via oxidative precipitation to Ce(IV) in the lower part of Bhs-podzols at the B/C interface, producing a positive Ce-anomaly in the oxalate soil extracts sampled from this zone ($Ce/Ce^* > 1$; Fig. 4h) while the soil solution containing the remaining REEs and having $Ce/Ce^* < 1$ continues to leach downslope. In the remainder of the catchment, REEs mobilized via weathering leach from upslope sources, especially following storm events, and are transported downslope where Ce is likewise deposited preferentially with respect to the other REEs in bimodal and Bh-podzols. We suggest that the REEs remaining in solution continue to migrate downgradient and leach into streams as drainage waters having $Ce/Ce^* < 1$ as the complement to preferential Ce deposition upslope.

Ce anomalies might be expected to increase with depth in most of the soil profiles due to decreasing acidity and increasing Fe oxide content, which favor precipitation of cerianite, Ce(IV) oxide (Braun et al., 1990; Vázquez-Ortega et al., 2015). Overall, however, there is no consistent pattern of increasing Ce anomaly magnitude with depth across the pedons sampled. Positive Ce anomalies in lower horizons (usually in a BC or CB horizon beneath spodic horizons) and downslope soils may indicate saturated and/or unsaturated lateral flow and depositional processes at the base of the solum. For example, in deeper horizons with less spodic materials along catena 2, Ce/Ce^* of approximately 2 to 8 probably resulted from lateral water flux documented in these zones by Gannon et al. (2017), though we note that overall Ce concentration was low relative to that in spodic horizons. On the other hand, significant Ce-anomalies were found in typical podzols below the spodic horizon in pedons 2.1 and 3.1 (Figs. 5 and 6). However, these pedons did not experience water table in the solum during the monitoring period (Supp. Fig. 4), and they likely had a predominantly unsaturated, vertical water regime that is characteristic of other typical podzols (Gannon et al., 2014). Therefore, it is possible that positive Ce/Ce^* below the spodic horizon in typical podzols developed due to unsaturated water movement and soil development. This hypothesis is evidenced by significant accumulations of Al_o below the spodic horizon in pedons 2.1 and 3.1 where positive Ce-anomalies were observed (Figs. 5 and 6).

Further evidence for the applicability of Ce/Ce^* as a hydropedologic tracer was the location of observed positive cerium anomaly “spikes” in upper horizons that corresponded to the top of the zone saturated by laterally flowing groundwater, which could form a redox interface for Ce. For example, there was a spike in Ce/Ce^* in pedon 2.4, a Bh-podzol, at 11 cm, which corresponded to the top of the Bh horizon (Fig. 5h; Supp. Table 1). Unfortunately, water table data for pedon 2.4 were lost due to equipment damage. However, Gannon et al. (2017) recorded water table and tensiometer data for a similar Bh-podzol in the same near-stream toeslope position several meters north of pedon 2.4 (part of Catena 2; Fig. 1). Following storm events, the highest water table observed in this nearby soil was at approx. 10 cm depth, but the water table would drain within a few days to between 40–50 cm depth and, above this zone, lateral unsaturated water flux was dominant (Gannon et al., 2017). It is likely that pedon 2.4 had similar water table dynamics and that the spike in Ce corresponded to the depth to highest water table and the zone of predominantly unsaturated water flux. Below the spike at 11 cm in pedon 2.4, Ce/Ce^* decreased between 11–40 cm, but then increased dramatically between 40–73 cm (Fig. 5h), where Ce/Ce^* likely increased due to deposition with laterally flowing, persistent groundwater. Pedon 2.4 contrasted with pedons 2.1 and 2.2 (typical podzols) with regard to the Ce/Ce^* depth profile (Fig. 5h), and these differences were interpreted to be due to the lack water table and dominantly vertical water flux in the upper profile, characteristic of typical podzols (Supp. Fig. 4b, Gannon et al., 2015; Gannon et al., 2017). Pedon 2.1 showed an increase in Ce/Ce^* with depth, but did not show any spikes higher in the profile and displayed Ce/Ce^* values lower than pedon 2.4 throughout most of the profile (Fig. 5h). However, because the Ce/Ce^* did increase with depth between 40–100 cm in pedon 2.1 (Fig. 5h), and because pedon 2.1 was located on a backslope (Fig. 3b), it is possible there was lateral unsaturated flow in the lower part and/or lateral deposition of from Ce delivered from a higher elevation that has accumulated at the B/C interface. Pedon 2.2 showed

more of a difference in Ce/Ce* between pedon 2.4, with an increase evident only between 85–100 cm, also possibly due to lateral redistribution of Ce at the B/C interface. A spike in Ce/Ce* in pedon 3.2 at 32 cm (Fig. 6h) could also correspond to the depth of seasonally high water table. Well data for pedon 3.3 (which was approx. 2 m from pedon 3.2) show an average water table depth between 30–40 cm (Supp. Fig. 4c). Pedon 3.3, a bimodal podzol, contrasted with pedon 3.1, a typical podzol that showed a near absence of water table during the monitoring period (Supp. Fig. 4c). Similar to what was observed for Catena 2, a lack of depth trend and relatively lower values for Ce/Ce* in pedon 3.1 compared to pedon 3.3 was likely due to a lack of both water table and lateral water flux.

The range of Ce/Ce* reported for soils elsewhere is generally only between 0.7–1.5 for a variety of locations (Braun et al., 1998; Savichev and Vodyanitskii, 2012; Vázquez-Ortega et al., 2015; Pedrot et al., 2015). Therefore, the magnitude of Ce-anomalies in WS3 appears to be much higher than others have reported. The existence of a positive Ce-anomaly in the soil implies that there must be a coupled negative Ce-anomaly somewhere in the ecosystem, either in the groundwater and stream water draining the catchment or in some as yet unidentified mineral weathering products remaining at the sites of REE mobilization to weathering solutions. Others have shown that a positive Ce-anomaly in soils can result in the production of a negative Ce-anomaly in the groundwater and stream water draining the soils (Seto and Akagi, 2008). It is possible that REEs are leached unfractionated from higher up in the catchment, and Ce is deposited preferentially downslope in Fe- and Mn-rich spodic materials while the remaining REEs continue to leach into the stream. Although measuring the Ce-anomaly in the waters of WS3 was beyond the scope of this study, this hypothesis could be tested in the future.

Cerium is similar to Mn in its redox reactivity, i.e., they are both oxidized or reduced under somewhat similar Eh/pH conditions. However, Ce persisted in the soils of WS3 while Mn was lost from the subsoil through leaching and/or vegetative uptake and subsequent enrichment of surface horizons with addition of Mn from plant residues. Like Mn, Ce is ubiquitous, but REEs are found in low concentrations in plants, since there is little transfer to plant tissues due to their large hydrated radius (Tyler, 2004). Therefore, Ce/Ce* may be a more consistent indicator of lateral flow than Mn_d/Fe_d, at least in the subsurface. In WS3, Ce/Ce* was also a better indicator of lateral flow than Fe_o/Fe_d, which followed vertical podzolization and showed no downslope trends (Supp. Fig. 3). The Ce-anomaly may also indicate other hydrologic and pedogenic processes, such as depth to seasonally high water table and incipient soil development below the B horizon.

Here we demonstrate that the spatial distribution of Ce-anomalies in oxalate extracts of podzols can provide a strong indication of lateral water flow and development of podzols along catenas. We suggest that the potential use of the Ce-anomaly as a hydropedologic tracer is not limited to supplementing data from existing hydrologic instrumentation. Indeed, the Ce-anomaly could possibly be used to help direct the initial instrumentation strategy and vision of fluxes for any catchment-scale study. For example, if several locations in a catchment were predicted to have lateral water flux based on topographic and morphological factors, the Ce-anomaly could be analyzed in the soils of the potential study sites. The presence or absence of large, positive Ce-anomalies and particularly the depth distribution of those anomalies across a suite of pedons would provide evidence of vertical vs. lateral flux and would help narrow down the selections for location of monitoring wells, tensiometers, etc. This pre-assessment of soil chemistry could theoretically be used to target specific soils for instrumentation that could yield representative data for the whole catchment. Performing oxalate extractions on soils is a straightforward technique, and there has been a proliferation of the ICP-mass spectrometry technology to measure REE abundances precisely. Therefore, we suggest that assessment of the spatial distribution of Ce anomalies in oxalate extracts of a subset of samples from soil profiles, from several carefully selected sites at key geomorphic positions in a catchment, could provide a useful reconnaissance tool that would guide further installation of hydrologic instrumentation specifically and catchment research design overall.

5. Conclusions

The functional soil types (hydropedologic units; HPUs) identified by Bailey et al. (2014) and Gannon et al. (2014) in Watershed 3 at Hubbard Brook Experimental Forest have significant differences with regards to pools of all major elements involved in podzolization: Fe_d, Mn_d, Fe_o, Al_o, and total organic C. Soil morphology was generally indicative of chemical composition. In general, soils with thicker spodic horizons had larger pools of metals and spodic C (subsoil organic C). Differences in subsurface water dynamics explain differences in chemical composition of the HPUs along catenas. In typical podzols dominated by vertical, unsaturated water flux, one finds vertical podzolization and intermediate-sized pools of elements associated with podzolization. E-podzols experience brief but intense lateral water flux, resulting in depletion of element pools; Bhs-podzols tend to have large pools of elements (especially Fe, Al, and spodic C) due to receipt of water and elements lost from E-podzols via lateral podzolization. Bimodal and Bh-podzols occur in near-stream or bench areas where they accumulate laterally translocated mobile elements (especially Mn and spodic C) due to a relatively persistent and high water table combined with unsaturated lateral flow. Despite the presence of high water table in some of the HPUs, they have some different characteristics and composition compared to the wetter, coarser-textured podzols of the Coastal Plain regions of warmer climates.

Certain naturally occurring elements can be used as hydropedologic indicators to predict subsurface flow paths and soil development. In WS3, a large positive Ce-anomaly (Ce/Ce*) at shallow to intermediate soil depths was indicative of lateral water flux and seasonally high water table. Vertical and lateral distribution of Ce/Ce* could potentially reveal hillslope-scale water movement in other catchments as well; this needs to be explored further. More commonly used elemental ratios (Mn_d/Fe_d and Fe_o/Fe_d) were not useful as hydropedologic indicators, likely due to vegetative uplift of Mn and the dominance of podzolization in determining the Fe active ratio.

Future studies of catchment biogeochemistry or hydrology should take predictable spatial variability of soil composition into account. Podzol development and chemistry are closely related to water table dynamics and may be used to predict parameters such as solute export. Given that global climate change is affecting water movement and distribution, development of podzols can be expected to change as well, and this warrants further understanding of the interactions of podzols with soil water and groundwater. In a broader sense, characterizing the spatial variability of any type of soils within a catchment improves understanding and prediction of ecosystem function and structure, and effects of headwater processes on ground water and stream water chemistry throughout larger catchments.

Supplementary data to this article can be found online at http://dx.doi.org/10.1016/j.geoderma.2017.05.039.

Acknowledgements

The authors wish to thank the following people for assistance in the field and laboratory: Noah Ahles, Andrea Brendalen, Margaret Burns, Silene DeCiucies, Cody Gillin, Ethan Morehouse, Emily Piché, Geoff Schwaner, and Margaret Zimmer. Thanks also to dissertation committee members Greg Druschel, Josef Görres, and Jeff Hughes for ideas and insight. Funding was provided by NSF Hydrologic Sciences (EAR 1014507) and LTER (DEB 1114804) programs. Hubbard Brook Experimental Forest is operated and maintained by the US Forest Service, Northern Research Station, Newtown Square, PA.

References

Bailey, S.W., Buso, D.C., Likens, G.E., 2003. Implications of sodium mass balance for interpreting the calcium cycle of a forested ecosystem. Ecology 84, 471–484.

Bailey, S., Brousseau, P., McGuire, K., Ross, D., 2014. Influence of hillslope position and transient water table on soil development and carbon distribution in a steep, headwater catchment. Geoderma 226-227, 279–289.

Bardy, M., Fritsch, E., Derenne, S., Allard, T., do Nascimento, N.R., Bueno, G.T., 2008. Micromorphology and spectroscopic characteristics of organic matter in waterlogged podzols of the upper Amazon basin. Geoderma 145, 222–230. http://dx.doi.org/10.1016/j.geoderma.2008.03.008.

Barrett, L., 1997. Podzolization under forest and stump prairie vegetation in northern Michigan. Geoderma 78, 37–58.

Blume, H.P., Schwertmann, U., 1969. Genetic evaluation of profile distribution of aluminum, iron, and manganese oxides. Soil Sci. Soc. Am. Proc. 33, 438–444.

Blumstock, M., Tetzlaff, D., Dick, J.J., Nuetzmann, G., Soulsby, C., 2016. Spatial organisation of groundwater dynamics and streamflow response from different hydropedological units in a montane catchment. Hydrol. Process. 30, 3735–3753. http://dx.doi.org/10.1002/hyp.10848.

Bourgault, R., 2014. Hydropedology of podzols at Hubbard Brook. (Ph.D. diss) Dept. of Plant and Soil Sci., University of Vermont, Burlington, VT.

Bourgault, R., Ross, D., Bailey, S., 2015a. Chemical and morphological distinctions between vertical and lateral podzolization at Hubbard Brook. Soil Sci. Soc. Am. J. 79, 428–439.

Bourgault, R., Ross, D., Bailey, S., 2015b. A response to “comment on ‘chemical and morphological distinctions between vertical and lateral podzolization at Hubbard Brook’ by Bourgault et al.”. Soil Sci. Soc. Am. J. 79, 1818.

Braun, J.-J., Pagel, M., Muller, J.-P., Bilong, P., Michard, A., Guillet, B., 1990. Cerium anomalies in lateritic profiles. Geochim. Cosmochim. Acta 54, 781–795.

Braun, J.-J., Viers, J., Dupre, B., Polve, M., Ndam, J., Muller, J.-P., 1998. Geochim. Cosmochim. Acta 62, 273–299.

Burns, M.A., 2012. The hydrological and geochemical role of the C horizon in a glacial till mantled headwater catchment. In: University of Maine Honors College, Paper 42, (http://digitalcommons.library.umaine.edu/honors/42).

Buurman, P., 1985. Carbon/sesquioxide ratios in organic complexes and the transition albic-spodic horizon. J. Soil Sci. 36, 255–260.

Buurman, P., Jongmans, A.G., 2005. Podzolisation and soil organic matter dynamics. Geoderma 125, 71–83.

Buurman, P., Vidal-Torrado, P., 2015. A comment on “chemical and morphological distinctions between vertical and lateral podzolization at Hubbard Brook” by Bourgault et al. Soil Sci. Soc. Am. J. 79, 1815–1817.

Buurman, P., Vidal-Torrado, P., Moreira Martins, V., 2013a. The podzol hydrosequence of Itaguare (Sao Paolo, Brazil). 1. Geomorphology and interpretation of profile morphology. Soil Sci. Soc. Am. J. 77, 1294–1306.

Buurman, P., Vidal-Torrado, P., Moreira Martins, V., 2013b. The podzol hydrosequence of Itaguare (Sao Paolo, Brazil). 1. Soil organic matter chemistry by pyrolysis-gas chromatography/mass spectrometry. Soil Sci. Soc. Am. J. 77, 1307–1318.

Cogger, C.G., Kennedy, P.E., 1992. Seasonally saturated soils in the Puget Lowland. I. Saturation, reduction, and color patterns. Soil Sci. 153, 421–433.

Courchesne, F., Turmel, M.-C., 2007. Extractable Al, Fe, Mn, and Si. In: Carter, M.R., Gregorich, E.G. (Eds.), Soil Sampling and Methods of Analysis, 2nd ed. CRC Press, Boca Raton, FL, pp. 307–315.

Crave, A., Gascuel-Odoux, C., 1997. The influence of topography on time and space distribution of soil surface water content. Hydrol. Process. 11, 203–210.

D'Amore, D.V., Fellman, J.B., Edwards, R.T., Hood, E., Ping, C.-L., 2012. Hydropedology of the North American coastal temperate rainforest. In: Lin, H. (Ed.), Hydropedology. Elsevier Academic Press, Boston, pp. 351–380.

D'Amore, D.V., Edwards, R.T., Herendeen, P.A., Hood, E., Fellman, J.B., 2015. Dissolved organic carbon fluxes from hydropedologic units in Alaskan coastal temperate rainforest watersheds. Soil Sci. Soc. Am. J. 79, 378–388.

Dib, A.E., Johnson, C.E., Driscoll, C.T., Fahey, T.J., Hayhoe, K., 2014. Simulating effects of changing climate and CO_2 emissions on soil carbon pools at the Hubbard Brook experimental forest. Glob. Chang. Biol. 20, 1643–1656.

Dore, M.H.I., 2005. Climate change and changes in global precipitation patterns: what do we know? Environ. Int. 31, 1167–1181.

Federer, C.A., Turcotte, D.E., Smith, C.T., 1993. The organic fraction-bulk density relationship and the expression of nutrient content in forest soils. Can. J. For. Res. 23, 1026–1032.

Feldman, S.B., Zelazny, L.W., Baker, J.C., 1991. High-elevation forest soils of the Southern Appalachians: II. Geomorphology, pedogenesis, and clay mineralogy. Soil Sci. Soc. Am. J. 55, 1782–1791.

Fiedler, S., Jungkunst, H.P.F., Jahn, R., Kleber, M., Sommer, M., Stahr, K., 2002. Linking soil classification and soil dynamics – pedological and ecological perspectives. J. Plant Nutr. Soil Sci. 165, 517–529.

Freeland, J.A., Evans, C.V., 1993. Genesis and profile development of success soils, northern New Hampshire. Soil Sci. Soc. Am. J. 57, 183–191.

Fritsch, E., Allard, T., Benedetti, M.F., Bardy, M., do Nascimento, N.R., Li, Y., Calas, G., 2009. Organic complexation and translocation of ferric iron in podzols of the Negro River watershed. Separation of secondary Fe species from Al species. Geochim. Cosmochim. Acta 73, 1813–1825.

Gannon, J.P., Bailey, S.W., McGuire, K.J., 2014. Organizing groundwater regimes and response thresholds by soils: a framework for understanding runoff generation in a headwater catchment. Water Resour. Res. 50, 8403–8419. http://dx.doi.org/10.1002/2014WR015498.

Gannon, J.P., Bailey, S.W., McGuire, K.J., Shanley, J.B., 2015. Flushing of distal hillslopes as an alternative source of stream dissolved organic carbon in a headwater catchment. Water Resour. Res. 51, 8114–8128.

Gannon, J.P., McGuire, K.J., Bailey, S.W., Bourgault, R.R., Ross, D.S., 2017. Lateral water flux in the unsaturated zone: a mechanism for the formation of spatial soil heterogeneity in a headwater catchment. Hydrol. Process. http://dx.doi.org/10.1002/hyp.11279.

Gillin, C.P., Bailey, S.W., McGuire, K.J., Gannon, J.P., 2015. Mapping of hydropedologic spatial patterns in a steep headwater catchment. Soil Sci. Soc. Am. J. 79, 440–453. http://dx.doi.org/10.2136/sssaj2014.05.0189.

Harris, W., 2001. Hydrologically linked Spodosol formation in the southeastern United States. In: Richardson, J., Vepraskas, M.J. (Eds.), Wetland Soils: Genesis, Hydrology, Landscapes, and Classification. CRC Press, Boca Raton, FL, pp. 331–342.

Harris, W.G., Hollien, K.A., 2000. Changes across artificial E-Bh boundaries generated under simulated fluctuating water tables. Soil Sci. Soc. Am. J. 64, 967–973.

Hjerdt, K.N., McDonnell, J.J., Seibert, J., Rodhe, A., 2004. A new topographic index to quantify downslope controls on local drainage. Water Resour. Res. 40, W05602. http://dx.doi.org/10.1029/2004WR003130.

Huntington, T.G., 2003. Climate warming could reduce runoff significantly in New England. Agric. For. Meteorol. 117, 193–201.

Jankowski, M., 2014. The evidence of lateral podzolization in sandy soils of Northern Poland. Catena 112, 139–147.

Jenny, H., 1946. Arrangement of soil series and types according to functions of soil-forming factors. Soil Sci. 61, 375–391.

Kuehl, R.J., Comerford, N.B., Brown, R.B., 1997. Aquods and psammaquents: problems in hydric soil identification. In: Vepraskas, M.J., Sprecher, S.W. (Eds.), Aquic Conditions and Hydric Soils: The Problem Soils. SSSA Spec. Publ 50. SSSA, Madison, WI, pp. 41–59.

Land, M., Öhlander, B., Ingri, J., Thunberg, J., 1999. Solid speciation and fractionation of rare earth elements in a Spodosol profile from northern Sweden as revealed by sequential extraction. Chem. Geol. 160, 121–138.

Laveuf, C., Cornu, S., 2009. A review on the potentiality of rare earth elements to trace pedogenetic processes. Geoderma 154, 1–12.

Li, S.-Y., Chen, Z.-S., Liu, J.-C., 1998. Subalpine loamy spodosols in Taiwan: characteristics, micromorphology, and genesis. Soil Sci. Soc. Am. J. 62, 710–716.

Likens, G.E., 2013. Biogeochemistry of A Forested Ecosystem, 3rd ed. Springer-Verlag, New York.

Lin, H., 2010. Linking principles of soil formation and flow regimes. J. Hydrol. 393, 3–19.

Löfgren, S., Cory, N., 2010. Groundwater Al dynamics in boreal hillslopes at three integrated monitoring sites along a sulphur deposition gradient in Sweden. J. Hydrol. 380, 289–297.

Lucas, Y., Montes, C.R., Mounier, S., Loustau Cazalet, M., Ishida, D., Achard, R., Garnier, C., Coulomb, B., Melfi, A.J., 2012. Biogeochemistry of an Amazonian podzol-ferralsol soil system with white kaolin. Biogeosciences 9, 3705–3720.

Lundstrom, U.S., van Breemen, N., Bain, D., 2000. The podzolization process. A review. Geoderma 94, 91–107.

Mapa, R.B., Pathmarajah, S., 2007. Contrasts in the physical properties of three soils of an Alfisol catena in Sri Lanka. Soil Use Manag. 11, 90–93.

McCord, J.T., Stephens, D.B., Wilson, J.L., 1991. Toward validating state-dependent macroscopic anisotropy in unsaturated media: field experiments and modeling considerations. J. Contam. Hydrol. 7, 145–175.

McDaniel, P.A., Bathke, G.R., Buol, S.W., Cassel, D.K., Falen, A.L., 1992. Secondary manganese/iron ratios as pedochemical indicators of field-scale throughflow water movement. Soil Sci. Soc. Am. J. 56, 1211–1217.

McKeague, J.A., DeConinck, F., Franzmeier, D.P., 1983. Spodosols. In: Wilding, L.P., Smeck, N.E., Hall, G.F. (Eds.), Pedogenesis and Soil Taxonomy: II. The Soil Orders. Elsevier, New York, pp. 217–252.

Melkerud, P.-A., Bain, D.C., Jongmans, A.G., Tarvainen, T., 2000. Chemical, mineralogical and morphological characterization of three podzols developed on glacial deposits in Northern Europe. Geoderma 94, 125–148.

Milne, G., 1947. A soil reconnaissance journey through part of Tanganyika Territory December 1935 to February 1936. J. Ecol. 35, 192–265. http://dx.doi.org/10.2307/2256508.

Mirus, B.B., 2015. Evaluating the importance of characterizing soil structure and horizons in parameterizing a hydrologic process model. Hydrol. Process. 29, 4611–4623.

Murray, R.W., Buchholtz Ten Brink, M.R., Brumsack, H.J., Gerlach, D.C., Russ III, G.P., 1991. Rare earth elements in Japan Sea sediments and diagenetic behavior of Ce/Ce*: results from ODP Leg 127. Geochim. Cosmochim. Acta 55, 2453–2466.

Park, S.J., Burt, T.P., 1999. Identification of throughflow using the distribution of secondary iron oxides in soils. Geoderma 93, 61–84.

Park, S.J., Burt, T.P., 2002. Identification and characterization of pedogeomorphological processes on a hillslope. Soil Sci. Soc. Am. J. 66, 1897–1910.

Pedrot, M., Dia, A., Davrance, M., Gruau, G., 2015. Upper soil horizons control the rare earth element patterns in shallow groundwater. Geoderma 239-240, 84–96.

Savichev, A., Vodyanitskii, Y., 2012. Improvement of the X-ray radiometric method of lanthanides diagnostics in soils. Eurasian Soil Sci. 45, 744–753.

Seto, M., Akagi, T., 2008. Chemical condition for the appearance of a negative Ce anomaly in stream waters and groundwaters. Geochem. J. 42, 371–380.

Sinai, G., Dirksen, C., 2006. Experimental evidence of lateral flow in unsaturated homogeneous isotropic sloping soil due to rainfall. Water Resour. Res. 42 (12).

Soil Survey Staff, 2004. Soil survey laboratory methods manual. In: Burt, R. (Ed.), Soil Survey Investigations Report No. 42, Ver. 4.0. U.S. Dept. of Agriculture, Natural Resources Conservation Service.

Soil Survey Staff, Natural Resources Conservation Service, United States Department of Agriculture, 2017. Official Soil Series Descriptions. (Available online. Accessed 05/13/2017).

Sommer, M., 2006. Influence of soil pattern on matter transport in and from terrestrial

biogeosystems – a new concept for landscape pedology. Geoderma 133, 107–123.
Sommer, M., Halm, D., Geisinger, C., Andruschkewitsch, I., Zarei, M., Stahr, K., 2001. Lateral podzolization in a sandstone catchment. Geoderma 103, 231–247.
Stolt, M.H., Rabenhorst, M.C., Ghabbour, E.A., Davies, G., 2016. Soil color and US Northeast aquods. Soil Sci. Soc. Am. J. http://dx.doi.org/10.2136/sssaj2015.11.0404.
Takahashi, Y., Shimizu, H., Usui, A., Kagi, H., Nomura, M., 2000. Direct observation of tetravalent cerium in ferromanganese nodules and crusts by X-ray-absorption near-edge structure (XANES). Geochim. Cosmochim. Acta 64, 2929–2935.
Tan, Z., Harris, W.G., Mansell, R.S., 1999. Water table dynamics across an Aquod-Udult transition in Florida flatwoods. Soil Sci. 164, 10–17.
Tebo, B.M., Johnson, H.A., McCarthy, J.K., Templeton, A.S., 2005. Geomicrobiology of manganese(II) oxidation. Trends Microbiol. 13, 421–428.
Tetzlaff, D., Birkel, C., Dick, J., Geris, J., Soulsby, C., 2014. Storage dynamics in hydropedological units control hillslope connectivity, runoff generation, and the evolution of catchment transit time distributions. Water Resour. Res. 50, 969–985.
Thomas, G.W., 1986. Soil pH and soil acidity. In: Sparks, D.L. (Ed.), Methods of Soil Analysis, Part 3: Chemical Methods. SSSA Book Series No. 5 Soil Science Society of America, Madison, WI, pp. 475–490.
Torres, R., Dietrich, W.E., Montgomery, D.R., Anderson, S.P., Loague, K., 1998. Unsaturated zone processes and the hydrologic response of a steep, unchanneled catchment. Water Resour. Res. 34, 1865–1879.
Tyler, G., 2004. Rare earth elements in soil and plant systems – a review. Plant Soil 267, 191–206.
Vázquez-Ortega, J., Perdrial, A., Harpold, X., Zapata-Rios, C., Rasmussen, J., McIntosh, M., Schaap, J., Pelletier, P., Brooks, M., Amistadi, K., Chorover, J., 2015. Rare earth elements as reactive tracers of biogeochemical weathering in forested rhyolitic terrain. Chem. Geol. 391, 19–32.
Vepraskas, M.J., 2001. Morphological features of seasonally reduced soils. In: Richardson, J., Vepraskas, M.J. (Eds.), Wetland Soils: Genesis, Hydrology, Landscapes, and Classification. CRC Press, Boca Raton, FL, pp. 331–342.
Weiler, M., McDonnell, J.J., Tromp-van Meerveld, I., Uchida, T., 2006. Subsurface stormflow. Encycl. Hydrol. Sci. 10, 112. http://dx.doi.org/10.1002/0470848944.hsa119.
Zaslavsky, D., Rogowski, A., 1969. Hydrologic and morphologic implications of anisotropy and infiltration in soil profile development. Soil Sci. Soc. Am. J. 33, 594–599.
Zimmer, M.A., Bailey, S.W., McGuire, K.J., Bullen, T.D., 2012. Fine scale variations of surface water chemistry in an ephemeral to perennial drainage network. Hydrol. Process. 27, 3438–3451.